

UDC 538.9; 539.2; 544.723

V.V. Turov¹, T.V. Krupska¹, M.D. Tsapko², V.M. Gun'ko¹

TEMPERATURE BEHAVIOR OF WATER AND *n*-DECANE BOUND TO NANOSILICA OR POLY(METHYLSILOXANE)

¹ *Chuiko Institute of Surface Chemistry of National Academy of Sciences of Ukraine
17 General Naumov Str., Kyiv, 03164, Ukraine, E-mail: vlad_gunko@ukr.net*

² *Taras Shevchenko National University of Kyiv, Faculty of Chemistry
60 Volodymyrska Str., Kyiv, 01601, Ukraine*

*The phase transition of *n*-decane bound to nanosilica initial hydrophilic or modified hydrophobic and branched 3D poly(methylsiloxane), PMS, was analyzed using ¹H NMR and quantum chemical methods. Freezing and melting points of *n*-decane are affected by nanosilica or PMS in CDCl₃ able to dissolve decane. The behavior of mixed water and decane depends on the adsorbent texture and surface nature, content of salt microparticles or nanoparticles and co-adsorbates. The freezing point depression under confined space results in stronger changes in the behavior of adsorbed decane than effects of melting delay occurring due to kinetic suppression and immobilization of solid-like structures in mesopores. The dispersion media (nonpolar CCl₄, weakly polar CDCl₃, polar CD₃CN and trifluoroacetic acid) influence the interfacial and temperature behavior of mixed water and *n*-decane because decane can be easily dissolved in nonpolar or weakly polar solvents but water can strongly interact with polar solvents and polar solid particles.*

Keywords: *poly(methylsiloxane), alkali metals chlorides, bound water and decane, interfacial behavior of water/decane mixture*

INTRODUCTION

The thermodynamic features of liquids and solutions depend on many factors, and temperature plays one of important roles [1]. They are especially specific close to temperature of phase transition of a solvent or a solute. This also depends on solubility of organics in water and vice versa. Additional important factor affecting the properties of liquids at the solid/liquid interfaces is the polarity or hydrophobicity and porosity of developed solid surface. To study features of liquids (e.g. their activity as solvents) at the interface, the amounts of liquids should be relatively low to avoid the masking effects of bulk liquids. Therefore in this paper, the interfacial behavior of water and *n*-decane (selected as a representative of hydrophobic liquids) is studied in the case of developed surfaces hydrophilic, partially hydrophilic/hydrophobic and hydrophobic in different dispersion media.

The temperature behavior of alkanes individual or as components of mixed liquids is of importance from practical point of view. For low-molecular weight alkanes, the phase transition occurs in a narrow temperature range. However, the interfacial behavior of alkanes confined in pores is

characterized by a certain freezing point depression [2–4]. This effect depends on both the properties of alkanes (e.g. molecular weights and structure of components) and the textural characteristics and surface chemistry of adsorbents. Salts located at the interfaces in the shape of dissolved ions or nanoparticles can strongly change the interfacial and temperature behavior of liquids located at the interfaces. For instance, cations K⁺ and anions Cl⁻ are chaotropes but Li⁺ and Na⁺ are kosmotropes differently affecting water structure [5, 6]. The cation influence on water structure increases with decreasing cation size and depends on the hydration degree. Jones-Dole viscosity *B* coefficients are equal to 0.15 (Li⁺) and 0.086 (Na⁺) for kosmotropes studied here, and -0.007 (K⁺, Cl⁻) for chaotropes [7, 8]. It is of interest to analyze the effects of cations of different univalent alkali Li⁺, Na⁺, and K⁺ on the behavior of the dispersion phase (nanosilica, PMS) and the characteristics of interfacial liquids (water, *n*-decane) affected by different dispersion media (air, water, nonpolar CCl₄, weakly polar chloroform alone or with addition of polar CD₃CN or strongly polar trifluoroacetic acid). Additionally, salt crystallites formed in pores can damage the materials that

depend on pore sizes, as well as on contents of salts and water [9].

NMR spectroscopy is a very effective method to study the interfacial phenomena [10–14], different organic and inorganic systems [15–21], water-hydrophobic organics [22–24], as well as biomaterials and more complex systems [25–28]. Previous investigations of the temperature behavior of *n*-decane and silicone oils bound to silica showed that their portions confined in pores remain liquid at temperatures lower than the freezing point $T < T_f$ [29, 30]. These effects are caused by several reasons. First, the freezing point depression is due to confined space effects as it is described by Gibbs-Thomson relation [31–33]. Second, kinetic hindrances of the phase transition in the interfacial layers, *i.e.* equilibration time becomes much longer than that for bulk liquids [34]. Third, partial freezing of adsorbates in pores enhances the confined space effects for a residual liquid fraction due to changes in the topology of pores. Additionally, polar or nonpolar liquid components, as well as dispersion media, can affect all these interfacial phenomena [29–34]. Thus, a significant portion of interfacial components located in pores can be in a liquid state during relatively long time and characterized by much longer time of transverse relaxation than a solid-like fraction. This effect allows the separation of ^1H NMR signals of liquid and solid-like fractions, since appropriate narrowing bandwidth allows the observation of signals of a liquid fraction only. Clearly, changes in the dispersion media (*e.g.* air, water, chloroform, *etc.*) or appearance of ions or polar nanoparticles can strongly change the temperature behavior of liquid mixtures [34].

The aim of this work is to study the temperature behavior of *n*-decane with the presence of water at a surface of hydrophilic initial pyrogenic silica PS300, hydrophobic silica HPS300, or partially hydrophilic (due to residual silanols) and partially hydrophobic (SiCH_3 groups) poly(methylsiloxane), PMS, alone or with crystallites of LiCl, NaCl, and KCl (grinded with nanosilica) in different dispersion media (CDCl_3 or CCl_4).

EXPERIMENTAL

Pyrogenic (fumed) silica PS300 and hydrophobic HPS300 produced with PS300 totally covered by trimethylsilyl groups (pilot plant of the Chuiko Institute of Surface Chemistry, Kalush, Ukraine, with the specific surface area of *ca.*

300 m^2/g), hydrated poly(methylsiloxane), PMS, Enterosgel (Kreoma-Pharm, Kiev, Ukraine), which composed of 10 wt. % of PMS and 90 wt. % of water (*i.e.* the hydration degree $h = 9$ g of water per 1 g of dry PMS) were used as the initial materials. Many of properties of fumed silica were described elsewhere [34–37], as well as PMS [38]. PMS in contrast to linear poly(dimethylsiloxane) is a branched 3D polymer which can be characterized by certain porosity of nanoparticles composed of folded macromolecules.

Salt/solids mixtures (3 : 1, 1 : 1, 1 : 3, or 1 : 6 w/w) were prepared by their grinding in a porcelain mortar. The powders were placed into 5 mm NMR ampoules and after adding water or (and) decane, CDCl_3 or CCl_4 was added as a dispersion medium. For some samples, acetonitrile or (and) trifluoroacetic acid (TFAA) was added. Notice that all concentrations shown below were calculated per gram of corresponding dry solids.

^1H NMR spectra of static samples were recorded using a Varian 400 Mercury spectrometer (magnetic field 9.4 T) utilizing 90° pulses of 3 μs duration. Each spectrum was recorded by coaddition of eight scans with a 2 s delay between each scan. Relative mean errors were less than $\pm 10\%$ for ^1H NMR signal intensity for overlapped signals, and $\pm 5\%$ for single signals. Temperature control by a Bruker VT-1000 device was accurate and precise to within ± 1 K. The accuracy of integral intensities was improved by compensating for phase distortion and zero line nonlinearity with the same intensity scale at different temperatures. Repeated measurements of samples gave identical spectra, within experimental error, at the same temperature. To prevent supercooling, spectra were recorded at $T = 210$ K (for samples precooled to this temperature for 10 min), then heated to 280 K at a rate of 5 K/min with steps $\Delta T = 10$ K or 5 K (with a heating rate of 5 K/min for 2 min), and maintained at a fixed temperature for 8 min for data acquisition at each temperature. The applications of this method and NMR cryoporometry to nanooxides were described in detail elsewhere [31–34].

The amount of unfrozen water (C_{uw}) as a function of temperature at $T < 273$ K was measured by comparing the total ^1H NMR integrated signal intensity of unfrozen water, I_{uw} , with that of all water at $T > 273$ K. This was done using a calibrated function $I_C = f(C_{\text{H}_2\text{O}})$, assuming $C_{\text{uw}} = C_{\text{H}_2\text{O}} I_{\text{uw}}/f(C_{\text{H}_2\text{O}})$. The function $f(C_{\text{H}_2\text{O}})$ was

determined by measurements of the total integral intensity of the ^1H NMR spectra after known amounts of water were added to the materials at $T > 273$ K. The low-temperature ^1H NMR spectroscopy provides structural information on interfacial water, pore structure (with cryoporometry and relaxometry), and thermodynamic characteristics of bound water or other liquids [31–34]. These characteristics include changes in Gibbs free energy caused by the adsorption (ΔG) of strongly bound water (SBW), $\Delta G_s < -0.5$ kJ/mol, and weakly bound water (WBW), $\Delta G_w > -0.5$ kJ/mol. In addition, the amounts of SBW (C_{uw}^s) and WBW (C_{uw}^w) can be obtained. WBW is frozen at $T > 255$ – 260 K while SBW is frozen at $T < 255$ – 260 K [34]. Furthermore, bound water can be assigned to strongly (SAW) or weakly (WAW) associated water based on the values of chemical shift. A $\delta_{\text{H}} = 4$ – 5 ppm indicates SAW with large 3D clusters or domains, chemical shifts of 1–2 ppm are indicative of WAW which consist of small 2D or strongly branched clusters.

According to the approximation of a Gibbs layer of finite thickness, surface forces act on a distance of several molecular layers. Changes in the Gibbs free energy of ice with temperature have been calculated as follows [34]:

$$\Delta G_{\text{ice}} = 0.0295 - 0.0413\Delta T + 6.64369 \times 10^{-5}(\Delta T)^2 + 2.27708 \times 10^{-8}(\Delta T)^3 \text{ (kJ/mol)}, \quad (1)$$

where $\Delta T = 273.16 - T$ at $T \leq 273.15$ K. Equation (1) was used to estimate the $\Delta G(T)$ function for bound water.

The freezing point depression for water in narrow pores is described by the Gibbs-Thomson relation (assuming a cylindrical pore shape) at radius R [31–34] given as Eq. (3):

$$\Delta T_m = T_{m,\infty} - T_m(R) = -\frac{2\sigma_{sl}T_{m,\infty}}{\Delta H_f \rho R} = \frac{k}{R}, \quad (2)$$

where $T_m(R)$ is the melting temperature of ice in cylindrical pores of radius R , $T_{m,\infty}$ the bulk melting temperature, ΔH_f the bulk enthalpy of fusion, ρ the density of the solid, σ_{sl} the energy of solid-liquid interaction, and k is a constant. Eq. (2) was used to determine the distribution function ($f_v(R) = dV_{\text{uw}}(R)/dR$) of sizes of water structures unfrozen at $T < 273$ K [15] and adsorbed onto nanosilicas. The $f_v(R)$ function can be used to determine the distribution function with respect to the specific surface area ($f_s(R)$) of water structures, and the size

distribution of pores (PSD) filled by this water [34]. Integration of the $f_s(R)$ function gives the specific surface (S_{uw}) of contact area between unfrozen water and a solid surface [34]. Such contributions can be differentiated as nanopores at $R \leq 1$ nm (S_{nano}), mesopores at $1 < R \leq 25$ nm (S_{meso}), and macropores at $R > 25$ nm (S_{macro}). Frequently, S_{uw} is less than S_{BET} due to partial filling of pores. Similar contributions to the pore volume can be calculated by integration of the $f_v(R)$ functions.

Quantum chemical calculations were carried out using *ab initio* and DFT methods with the 6-31G(d,p) basis set, using the Gaussian 09 [39] program suit, to full geometry optimization of molecules or clusters. The δ_{H} values were calculated as the difference in the isotropic values of the magnetic shielding tensors of H atoms ($\sigma_{\text{H,iso}}$) of tetramethylsilane, TMS ($\delta_{\text{H,TMS}} = 0$ ppm) as a reference compound ($\sigma_{\text{H,iso}} = 31.76$ ppm for TMS by GIAO/B3LYP/6-31G(d,p)) and a given compound using equation

$$\delta_{\text{H}} = \frac{1}{3} \text{Tr} \sigma_{\text{TMS}} - \frac{1}{3} \text{Tr} \sigma_{\text{H}}, \quad (3)$$

where Tr is the trace of matrix, since σ is the tensor with nine elements. The gauge-independent atomic orbital (GIAO) method [39] with the DFT method (B3LYP) and the 6-31G(d,p) basis set was used for a short PDMS molecule (seven units) and *n*-decane. The distribution functions of the δ_{H} values were calculated using a simple equation

$$f(\delta_{\text{H}}) = (2\pi\sigma^2)^{-0.5} \sum_j \exp[-(\delta_j - \delta_{\text{H}})^2 / 2\sigma^2], \quad (4)$$

where j is a number of H atom, σ^2 is the distribution dispersion, and δ_j is the calculated value of the j -th H atom. Large structures (up to 6000 atoms) were calculated using the PM7 method (MOPAC 2012 package with GPU/CUDA) [40, 41]. To calculate the $f(\delta_{\text{H}})$ functions using the PM7 results, a calibration function was used to describe the dependence between atomic charges q_{H} (PM7) and the δ_{H} values (GIAO/B3LYP/6-31G(d,p)) for the PDMS molecule with seven units. The solvation model SMD [42] was used with B3LYP/6-31G(d) method (WinGAMESS, version of 1 May 2013 (R1) [43]).

RESULTS AND DISCUSSION

During grinding salt (KCl was selected as a color representative) with strongly hydrated

PMS at $h = 9$ g/g (Fig. 1 *a, b*) or more weakly hydrated nanosilica at $h = 0.1$ g/g (Fig. 1 *c, d*) KCl microcrystallites are observed. A low content of water cannot allow the dissolution of salts. Their sizes are smaller in KCl/PS300 ($d \leq 5$ μm) than KCl/PMS ($d \leq 20$ μm) because

of an abrasive effect of nanosilica, which is much harder than the polymer used. Additionally, the KCl/PS300 has uniform color that suggests a uniform distribution of KCl particles in the mixture.

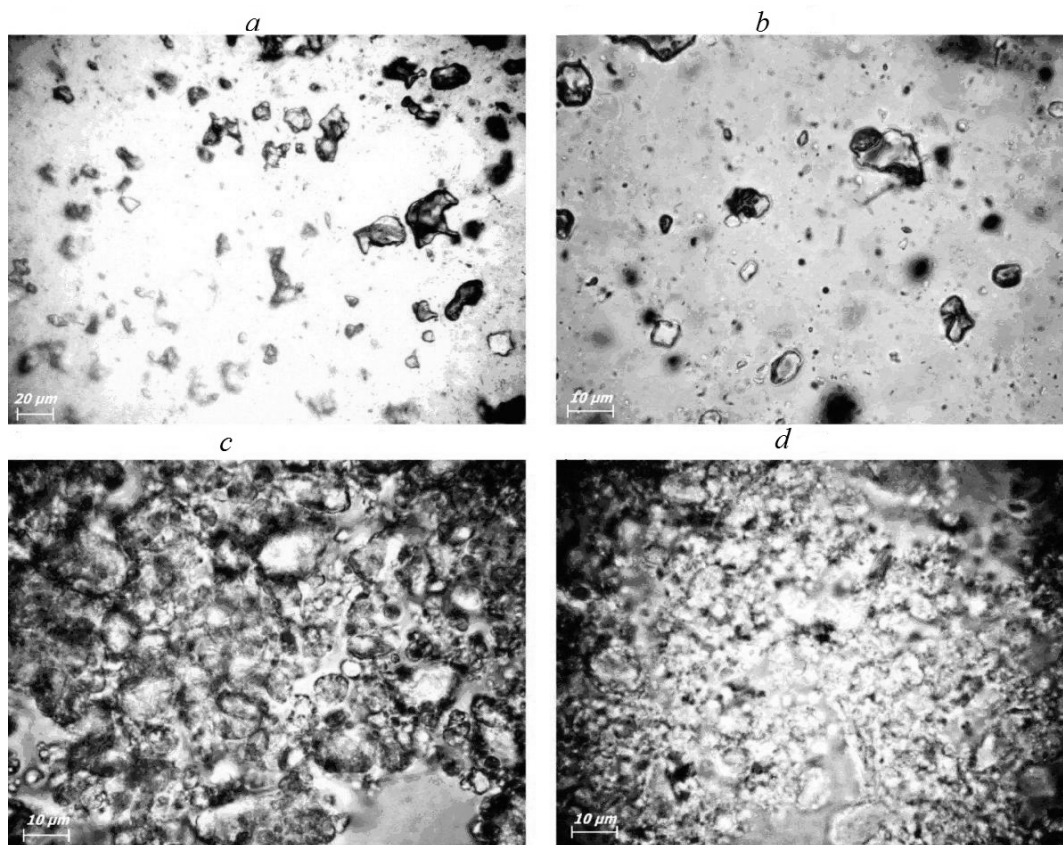


Fig. 1. Microphotographs (Primo Star optical microscope, Carl Zeiss) of grinded samples (during 10 min) (*a, b*) hydrated PMS ($h = 9$ g/g) with KCl (1 : 3 w/w) and (*c, d*) KCl/PS300 (1:6) at $h = 0.1$ g/g in (*c*) air and (*d*) silicone oil (scale bar 20 μm (*a*), and 10 μm (*b, c, d*))

Water bound to NaCl with the presence of *n*-decane shows a broad signal at $\delta_{\text{H}} \approx 4.5$ ppm at 280 K (Fig. 2 *a*, dash-dotted lines). At 270 K, its intensity becomes much lower and it disappears at 265 K due to freezing of water. This suggests that all water is weakly bound (WBW) because it is frozen close to the freezing point of bulk water. This water is strongly associated (SAW) since δ_{H} is close to that of bulk water [34]. Decane gives two signals at $\delta_{\text{H}} = 0.95$ ppm (CH_3 groups) and 1.25 ppm (CH_2) (Fig. 2 *a*). At low temperatures, a weak signal at 1.5–2.0 ppm can be assigned to weakly associated water (WAW). Addition of a certain amount of TFAA to chloroform (1:9) leads to a downfield shift of signal of TFAA/water toward 7–8 ppm. It is broad at high temperatures

and shifts toward 10 ppm with decreasing temperature close to that for bulk TFAA solution (~ 11 ppm).

A decrease in the content of decane and addition of KCl to hydrated PMS result in unexpected upfield shift of water signal from 5–6 ppm (dash-dotted lines) toward 4.5–5.0 ppm (solid lines, Fig. 2 *b*). This result can be explained by diminution of sizes of bound water structures after addition of KCl (Fig. 3 *b, c*). In contrast to the systems with NaCl (Fig. 2 *a*), signals of water and decane are not observed at $T < T_{\text{f,d}} = 243.5$ K (freezing point of bulk *n*-decane) (Fig. 2 *b*). However, in the presence of KCl signal of water is observed at 250–260 K. Thus, a small fraction of SAW is strongly bound, and signal of WAW

disappears at low temperatures even at $T < T_{f,d}$. Certain broadening of decane signal can be due to nonuniformity of magnetic susceptibility of samples including relatively large solid particles of salts.

Despite a relatively small amount of water (insufficient to dissolve NaCl in the studied samples) bound to NaCl particles, water forms relatively large structures at $R > 3$ nm in radius (Fig. 3 *a*). They correspond to SAW but WBW, since surface area of relatively large NaCl crystallites (Fig. 1) is small. Water bound to PMS, which is characterized by developed surface area ~ 200 m²/g [38], forms much smaller structures (Fig. 3 *b, c*), which correspond to both SBW and WBW, as well as SAW and WAW (Fig. 2 *b*). Addition of KCl leads to diminution of sizes of these structures (Fig. 3 *c*).

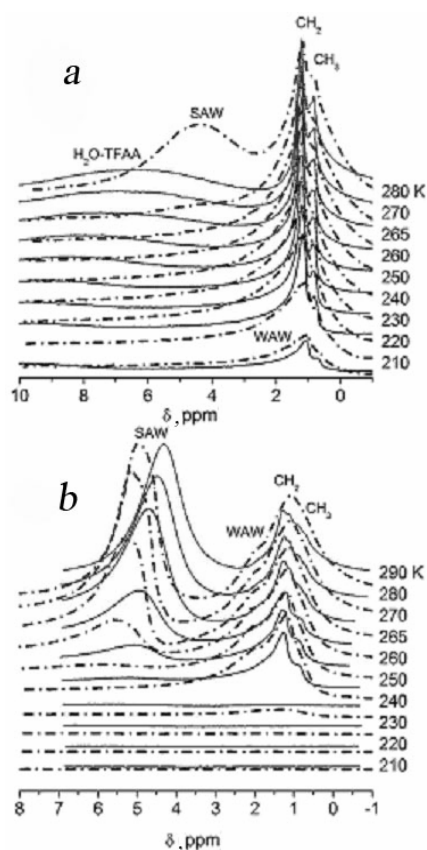


Fig. 2. ¹H NMR spectra recorded at different temperatures of water and *n*-decane bound to the NaCl powder in (a) CDCl₃ (dash-dotted lines) and CDCl₃/TFAA (9:1) (solid lines) at 0.1 g/g of water and 0.1 g/g of decane; (b) a mixture of hydrated PMS ($h = 9$ g/g) with decane (1 : 1) (dash-dotted lines) and a mixture with hydrated PMS/KCl (1 : 3) at $h = 9$ g/g and decane (4 : 1) (solid lines)

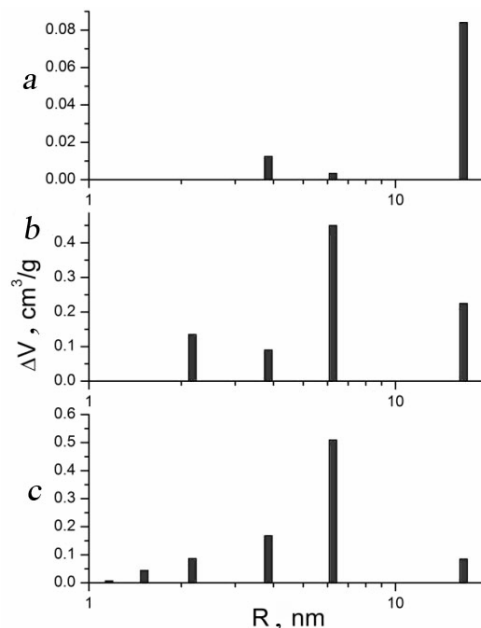


Fig. 3. Size distributions of unfrozen water structures in (a) NaCl powder with 0.1 g/g of water and 0.1 g/g decane in CDCl₃ medium; (b) hydrated PMS (90 wt. % water) with decane (1 : 1); and (c) a mixture with hydrated PMS/KCl (1 : 3) and decane (4 : 1)

In a mixture of PS300 nanoparticles with small KCl particles being in air, the freezing point depression is observed for both bound water and decane (Fig. 4 *a*). Unfrozen water is observed even at 210 K and decane at 220 K. Water forms relatively small structures (Fig. 5 *a*) in narrow voids between silica and salt particles. In CDCl₃ medium, lines become narrower (due to diminution of molecular exchange effects) (Fig. 4 *b*). A portion of water is displaced from pores.

This leads to differentiation of signals, since two signals of SAW are observed at $\delta_H = 5$ ppm (SAW1) and 3.5 ppm (SAW2), as well as WAW at $\delta_H = 1.7$ –2.0 ppm. Addition of CD₃CN to this mixture (Fig. 4 *c*) causes an upfield shift of water signals and a relative increase in the amounts of SAW2 and a decrease in the content of SAW1. This suggests decreasing associativity of bound water molecules. Addition of TFAA (Fig. 4 *d*) results in simplification and averaging of the spectra due to fast proton exchange between molecules of water and TFAA. Intensive signal of the aqueous solution of TFAA is observed at 10 ppm. Replace of NaCl by KCl (Fig. 4 *e*) or LiCl (Fig. 4 *f*) leads to enhancement of SAW1, including both SBW and WBW. Appearance of these waters corresponds to the formation of relatively small structures (Fig. 5 *c, d*).

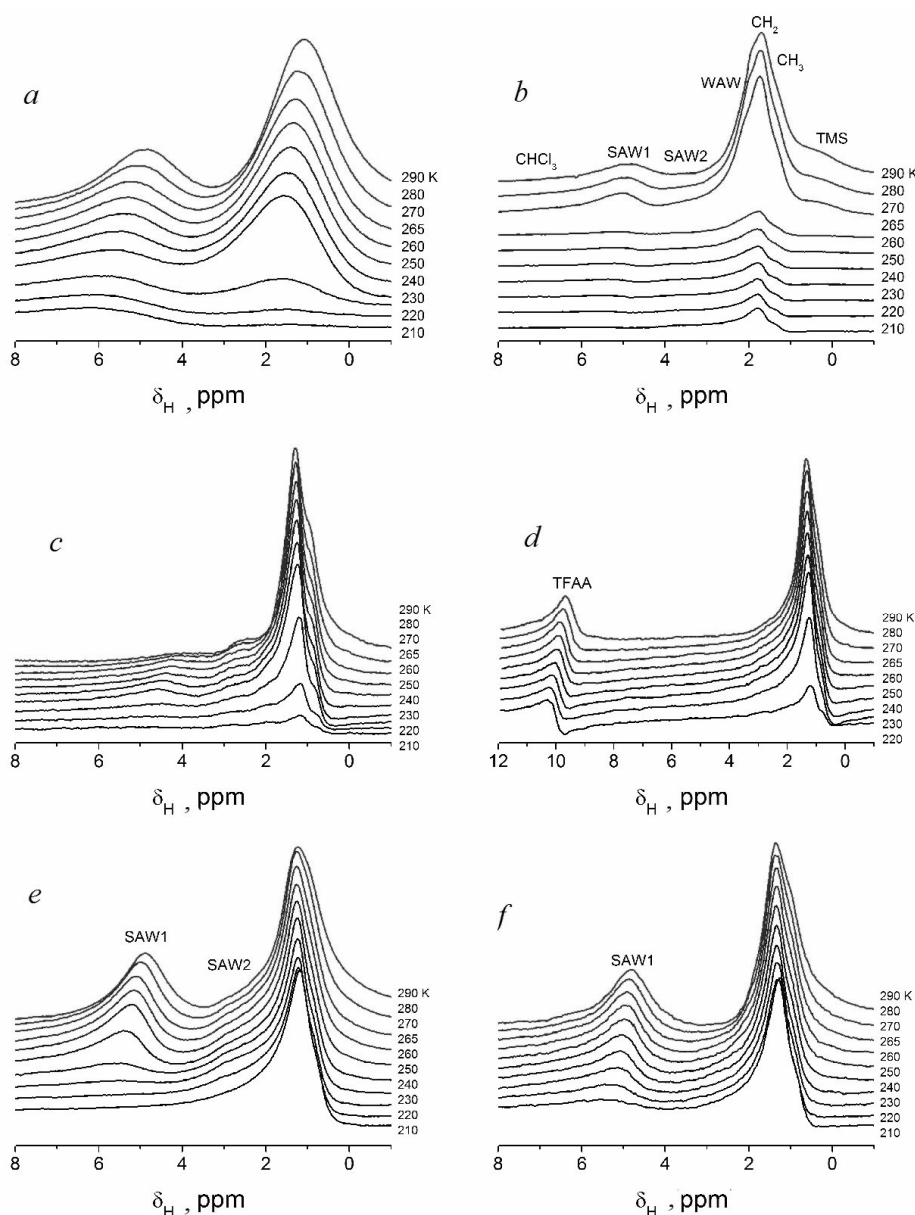


Fig. 4. ^1H NMR spectra recorded at different temperatures of water and *n*-decane bound to (a) PS300/KCl (6 : 1) at $h = 0.1$ g/g and $C_d = 0.2$ g/g in air; (b) PS300/KCl (6 : 1) at $h = 0.1$ g/g in a mixture with $\text{CDCl}_3/\text{C}_{10}\text{H}_{22}$ (7 : 1); (c) PS300/NaCl (6 : 1) at $h = 0.1$ g/g and $C_d = 0.15$ g/g in a mixture $\text{CDCl}_3/\text{CD}_3\text{CN}$ (4:1) medium; (d) PS300/NaCl (6 : 1) at $h = 0.1$ g/g and $C_d = 0.15$ g/g in a mixture $\text{CDCl}_3/\text{CD}_3\text{CN}/\text{TFAA}$ (4:1:1) medium (e) PS300/KCl (6 : 1) at $h = 0.1$ g/g and $C_d = 0.2$ g/g in CDCl_3 medium; and (f) PS300/LiCl (1 : 1) at $h = 0.1$ g/g and $C_d = 0.15$ g/g in CDCl_3 medium

The interfacial behavior of bound decane depends on the type of adsorbents (silica PS300 and HPS300, PMS, salts), the presence of water, and the type of dispersion medium. All these features reflect in the changes in the amounts of unfrozen decane vs. temperature recorded at increasing temperature from 210 K to 290 K (Fig. 6). At $I/I_0 = 0$, all decane is in solid-like state (freezing point $T_{f,d} = 243.5$ K), and at $I/I_0 = 1$, all decane is liquid.

The I/I_0 curves for decane bound to PMS (Fig. 6 a, curves 3 and 4) show a weak influence of hydrated PMS on the temperature behavior of decane that is similar to bulk decane. Consequently, decane cannot displace water from the PMS surface, since the confined space effects for decane are practically absent. For all other systems, the confined space effects are observed because a fraction of unfrozen decane is observed at $T < T_{f,d}$. There is another

effect of inhibition of melting a fraction of solid-like decane at $T > T_{f,d}$. This effect is maximal for decane bound to PS300/NaCl located in the CDCl_3 medium (Fig. 6 *b*, curve 1). This immobilization of bound decane can be maximal effective in mesopores of appropriate sizes. PS300 possesses textural mesopores and macropores [34]. During any treatment (grinding, suspending/drying, gelation, mechanochemical activation) of PS300, it becomes more compacted and its bulk density strongly increases (up to 0.3 g/cm^3), and this leads to increase in contributions of textural mesopores [34, 38, 44, 45]. A fraction of solid-like structures of decane formed in mesopores can remain during heating at $T > T_{f,d}$ because the heating rate is relatively high. This leads to delay in melting of bound structures. Notice that the I/I_0 curves for the systems with CDCl_3 dispersion medium are located lower than that for the systems in air (Fig. 6). In both air and CDCl_3 medium at $T \approx T_{f,d}$, approximately 70 % of decane is in a liquid state (Fig. 6). This shows a strong colligative effect of solvents with lower freezing point than that of solutes [4, 34].

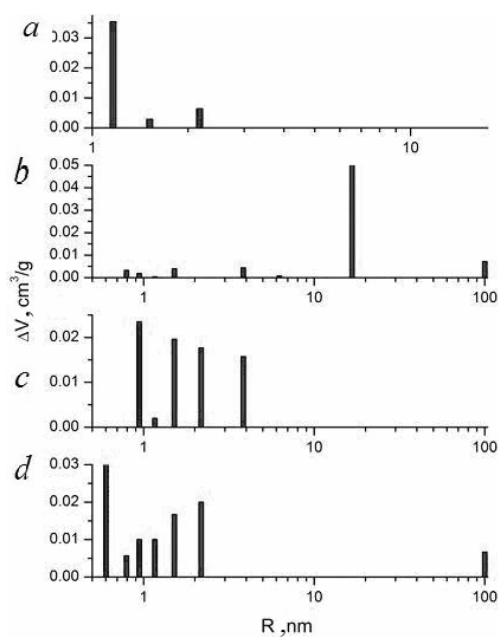


Fig. 5. Size distributions of unfrozen water structures in (a) PS300/KCl (6:1) in air; (b) PS300/NaCl (6:1) in CDCl_3 ; (c) PS300/KCl (6:1) in CDCl_3 ; and (d) PS300/LiCl (1:1) in CDCl_3

Table 1. Sample characteristics and integrated changes in the temperature range of phase transition of *n*-decane

Solids	H , g/g	C_d , g/g	Medium	Ψ_- , K	Ψ_+ , K	I/I_0 $T = T_f$
NaCl	0.15	0.1	CDCl_3	-17.8	5.1	0.73
NaCl	0.15	0.1	$5\text{CDCl}_3 + 1\text{TFAA}$	-17.8	9.0	0.71
PMS	9.0	1.0	Air	-1.7	4.2	0.40
1PMS/3KCl	9.0	0.23	Air	-1.5	3.4	0.35
6PS300/1KCl	0.1	0.20	Air	-7.9	6.5	0.73
6PS300/1NaCl	0.1	0.15	CDCl_3	-3.7	20.8	0.11
6PS300/1NaCl	0.1	0.15	$4\text{CDCl}_3 + 1\text{CD}_3\text{CN} + 1\text{TFAA}$	-12.7	8.7	0.77
6PS300/1KCl	0.1	0.20	CDCl_3	-21.3	7.3	0.68
PS300/LiCl	0.1	0.15	CDCl_3	-14.8	5.6	0.65
HPS300/KCl	0.1	0.10	CCl_4	-18.9	2.9	0.83

Note. $\Psi_- = \int_{T_{\min}}^{T_f} I(T)/I_0 dT$ and $\Psi_+ = \int_{T_f}^{T_{\max}} \frac{I_0 - I(T)}{I_0} dT$.

Minimal integrated effects on melting of decane are observed for the PMS systems (Table 1, ψ). This due to filling of pores by water ($h = 9 \text{ g/g}$), relative hydrophilicity of PMS due to the presence of a number of residual silanols [38], and relatively large sizes of KCl crystallites (Fig. 1). Notice that the maximal difference in changes in the Gibbs free energy of solvation of non-dissociated is for LiCl. Calculations with SMD/B3LYP/6-31G(d,p) clusters $\text{M}_{10}\text{Cl}_{10}$ ($M = \text{Li}, \text{Na}$) and K_8Cl_8 with the

geometry optimized using the HF/6-31G(d,p) method give for solvation in water and *n*-decane, respectively: -41.3 and -34.9 kJ/mol ($\text{Li}_{10}\text{Cl}_{10}$), -28.2 and -24.9 kJ/mol ($\text{Na}_{10}\text{Cl}_{10}$), and -22.5 and -18.2 kJ/mol (K_8Cl_8).

Thus, the difference for KCl particles in solvation by water and decane adds a reason to form large decane structures (bound to PMS/KCl) with the properties close to those of bulk decane. A significant decrease in the amounts of water from h

= 9 g/g bound to PMS to 0.1–0.15 g/g bound to silica with salts or individual NaCl leads to enhancement of the interfacial effects on decane (Table 1, ψ). In many cases, the freezing point depression effects (i.e. ψ_-) are stronger than the melting delay effects (i.e. ψ_+). Both effects depend more strongly on the textural characteristics and the amounts of water (i.e. filling of pores by water) than the types of silica and salts.

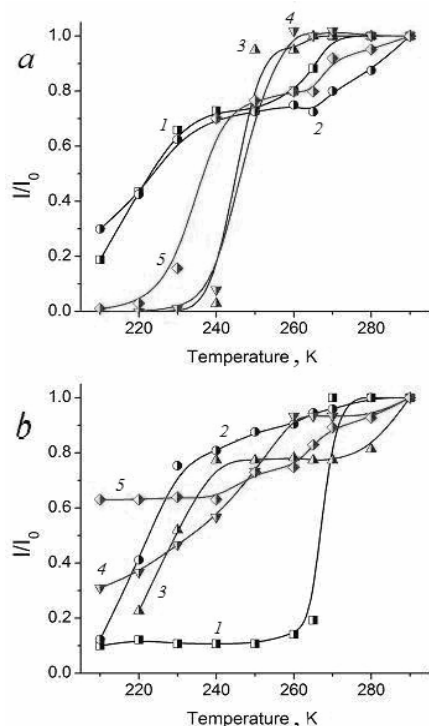


Fig. 6. Relative intensity in the 1H NMR spectra of decane (I_0 corresponds to intensity at 290 K) bound to (a) NaCl at $C_d=0.1$ g/g and $h=0.1$ g/g in $CDCl_3$ (curve 1), with added TFAA as $CDCl_3/TFAA=5:1$ (2); PMS/KCl (1:3) at $C_d=0.225$ g/g and $h=9$ g/g (3); PMS at $C_d=1$ g/g and $h=9$ g/g (4); and PS300/KCl (6:1) at $C_d=0.2$ g/g and $h=0.1$ g/g in air (5); (b) PS300/NaCl (6:1) at $C_d=0.15$ g/g and $h=0.1$ g/g in $CDCl_3$ (curve 1); HPS300/KCl (1:1) at $C_d=0.1$ g/g and $h=0.1$ g/g in CCl_4 (2); PS300/NaCl (6:1) at $C_d=0.15$ g/g and $h=0.1$ g/g in $CDCl_3/CD_3CN/TFAA$ (4:1:1) (3); PS300/LiCl (1:1) at $C_d=0.15$ g/g and $h=0.1$ g/g in $CDCl_3$ (4); and PS300/KCl (6:1) at $C_d=0.2$ g/g and $h=0.1$ g/g in $CDCl_3$ (5)

The latter can be explained by relatively weak effects of salt crystallites or dissolved ions on the 1H NMR spectra of water without of adsorbents (Fig. 7) or bound to silica (Fig. 8) because all the spectra are characterized by a signal at 4–5 ppm typically observed for bound SAW (Figs. 2 and 4)

or bulk water [34]. The spectrum of hydrated LiCl nanoparticles is slightly different due to partial dissolution of LiCl and formation of charged particles including H_3O^+ and OH^- . Anions Cl^- are chaotropes but cations Li^+ are kosmotropes, which differently affect the water structure, especially at a surface of polar nanoparticles. The dissolution effects are much weaker for NaCl nanoparticles (Fig. 7, curve 2). However, some separated fragments are formed (see insert in Fig. 7).

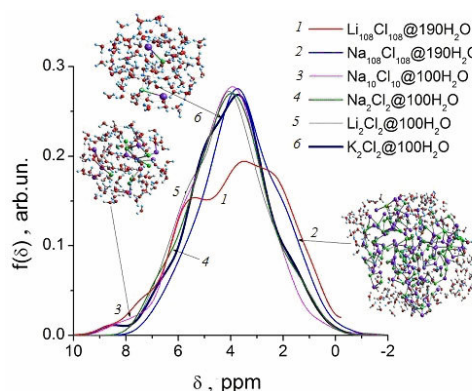


Fig. 7. Semiempirical PM7 calculations of the 1H chemical shifts of water with salt crystallites (curves 1–3) or dissolved ions (curves 4–6)

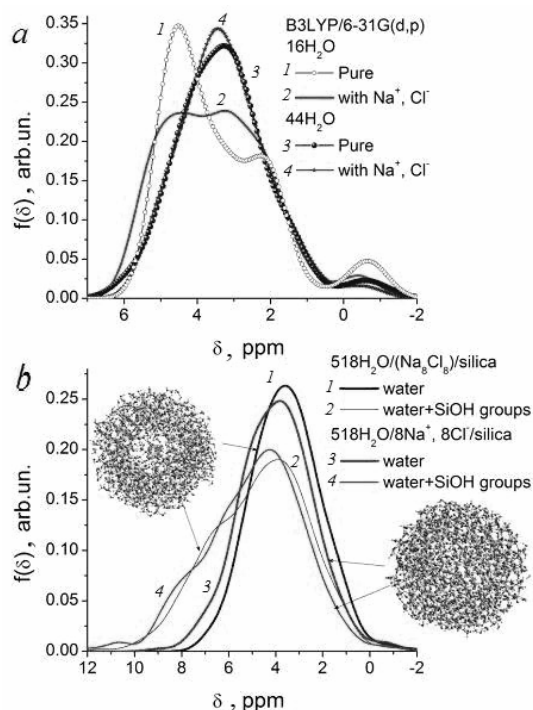


Fig. 8. (a) DFT B3LYP/6-31G(d,p) and (b) semiempirical PM7 calculations of the 1H chemical shifts in pure water, water with NaCl (a) alone or (b) bound to silica surface

CONCLUSION

The interfacial and temperature behavior of mixed water and *n*-decane depends on such several factors as the texture and surface nature of adsorbents, the presence and content of microparticles or nanoparticles of salts, the amounts of components. If water completely fills pores of poly(methylsiloxane), which contains both non-polar Si-CH₃ and polar Si-OH groups, that decane co-adsorbed onto already hydrated PMS practically does not sense the confined space effects and its freezing/melting occurs near the freezing point of bulk decane. If co-adsorbed water and decane fills only a portion of pores that their interfacial and temperature behavior depends on the texture of the adsorbents and amounts of salt crystallites. This leads to broadening of the temperature range of melting of decane in both sides from the freezing point of bulk decane. Typically, the freezing point depression due to confined space effects results in stronger changes

in the temperature behavior of adsorbed decane than the effects of melting delay due to both kinetic suppression and immobilization of solid-like structures of decane in mesopores of adsorbents. The dispersion media (nonpolar CCl₄, weakly polar CDCl₃, polar CD₃CN and TFAA) influence the interfacial and temperature behavior of co-adsorbed water and *n*-decane because decane can be easily dissolved in non-polar or weakly polar solvents but water can strongly interacts with polar solvents. This causes additional differentiation of the interfacial structures with water (including its four types SAW & WAW, SBW & WBW) and decane.

Acknowledgement. The authors are grateful to European Community, Seventh Framework Programme (FP7/2007–2013), Marie Curie International Research Staff Exchange Scheme (IRSES grants No 230790 and 612484) for financial support.

Температурна поведінка води та *n*-декану, зв'язаних нанокремнеземом або поліметилсилоксаном

В.В. Туров, Т.В. Крупська, М.Д. Цапко, В.М. Гунько

*Інститут хімії поверхні ім. О.О. Чуйка Національної академії наук України
вул. Генерала Наумова, 17, Київ, 03164, Україна, vlad_gunko@ukr.net
Київський національний університет імені Тараса Шевченка, Хімічний факультет
вул. Володимирська, 60, Київ, 01601, Україна*

*Фазові переходи *n*-декану, зв'язаного нанокремнеземом, вихідним гідрофільним або модифікованим гідрофобним, і розгалуженим 3D полі(метилсилоксаном), ПМС, проаналізовано з використанням ¹H ЯМР спектроскопії та квантовохімічних методів. Точки замерзання і плавлення *n*-декану залежать від дії нанокремнезему або ПМС в середовищі CDCl₃, яке здатне розчиняти декан. Поведінка суміші води і декану залежить від текстури та будови поверхні адсорбентів, вмісту мікрочастинок солі та ко-адсорбатів. Зниження точки замерзання декану у обмеженому просторі істотніше, ніж затримка його плавлення внаслідок кінетичних ефектів та іммобілізації в мезопорах заморожених структур. Дисперсійне середовище (неполярний CCl₄, слабкополярний CDCl₃, полярні CD₃CN і трифтороцтова кислота) впливає на температурну поведінку на межі поділу сумішей води та декану, оскільки декан може легко розчинятися в неполярних або слабкополярних розчинниках, а вода може сильно взаємодіяти з полярними розчинниками та полярними твердими наночастинами.*

Ключові слова: поліметилсилоксан, хлориди лужних металів, зв'язані вода та декан, поведінка на межі поділу сумішей води та декану

Температурное поведение воды и *n*-декана, связанных нанокремнеземом
или полиметилсилоксаном

В.В. Туров, Т.В. Крупская, М.Д. Цапко, В.М. Гунько

Институт химии поверхности им. А.А. Чуйко Национальной академии наук Украины
ул. Генерала Наумова, 17, Киев, 03164, Украина, vlad_gunko@ukr.net
Киевский национальный университет имени Тараса Шевченко, Химический факультет
ул. Владимирская, 60, Киев, 01601, Украина

Фазовые переходы *n*-декана, связанного нанокремнеземом, исходным гидрофильным или модифицированным гидрофобным, и разветвленным 3D поли(метилсилоксаном), ПМС, проанализировано с использованием ЯМР ^1H спектроскопии и квантовохимических методов. Точки замерзания и плавления *n*-декана зависят от действия нанокремнезема или ПМС в среде CDCl_3 , которая способна растворять декан. Поведение смесей воды и декана зависит от текстуры и строения поверхности адсорбентов, содержания микрочастиц соли и ко-адсорбатов. Снижение точки замерзания декана в ограниченном пространстве существенней, чем задержка его плавления вследствие кинетических эффектов и иммобилизации в мезопорах замороженных структур. Дисперсионная среда (неполярный CCl_4 , слабополярный CDCl_3 , полярный CD_3CN и трифторуксусная кислота) оказывает влияние на температурное поведение на границах раздела смесей воды и декана, поскольку декан может легко растворяться в неполярных или слабополярных растворителях, а вода может сильно взаимодействовать с полярными растворителями и полярными твердыми наночастицами.

Ключевые слова: полиметилсилоксан, хлориды щелочных металлов, связанные вода и декан, поведение на границах раздела смесей воды и декана

REFERENCES

1. Emmerich W. Chemical thermodynamics: A journey of many vistas, *J. Solution Chem.*, 43 (2014) 526.
2. Affens W.A., Hall J.M., Holt S., Hazlett R.N. Effect of composition on freezing points of model hydrocarbon fuels, *Fuel*, 63 (1984) 543.
3. Moynihan C.T., Shahriari M.R., Bardakci T. Thermal analysis of melting and freezing of jet and diesel fuels, *Thermochimica Acta*, 52 (1982) 131.
4. Jahromi S.G., Khodaii A. Effects of nanoclay on rheological properties of bitumen binder, *Construction and Building Materials*, 23 (2009) 2894.
5. Chaplin M. Water structure and science, <http://www.lsbu.ac.uk/water/>.
6. Kunz W. (ed.), *Specific Ion Effects*. World Scientific Publishing Co. Pte. Ltd., Singapore, 2009, 346 p.
7. Collins K.D. Ions from the Hofmeister series and osmolytes: Effects on proteins in solution and in the crystallization process, *Methods*, 34 (2004) 300.
8. Robinson J.B.Jr., Strottmann J.M., Stellwagen E. *Proc. Natl. Acad. Sci. USA*, 78 (1981) 2287.
9. Gupta S., Pel L., Kopinga K. Crystallization behavior of NaCl droplet during repeated crystallization and dissolution cycles: An NMR study, *Journal of Crystal Growth*, 391 (2014) 64.
10. Simpson A.J., McNally D.J., Simpson M.J. NMR spectroscopy in environmental research: from molecular interactions to global processes, *Prog. Nucl. Magn. Reson. Spectrosc.*, 58 (2011) 97.
11. Gerathanassis I.P. Oxygen-17 NMR spectroscopy: basic principles and applications. Part II, *Prog. Nucl. Magn. Reson. Spectrosc.*, 57 (2010) 1.
12. Demangeat J.-L. Nanosized solvent superstructures in ultramolecular aqueous dilutions: twenty years' research using water proton NMR relaxation, *Homeopathy*, 102 (2013) 87.
13. Koptyug I.V. MRI of mass transport in porous media: drying and sorption processes, *Prog. Nucl. Magn. Reson. Spectrosc.*, 65 (2012) 1.

14. Kasian N., Verheyen E., Vanbutsele G. et al. Catalytic activity of germanosilicate UTL zeolite in bifunctional hydroisomerisation of *n*-decane, *Microporous Mesoporous Mater.*, 166 (2013) 153.
15. Davarpanah L., Vahabzadeh F. Formation of oil-in-water (O/W) pickering emulsions via complexation between β -cyclodextrin and selected organic solvents, *Starch*, 64 (2012) 898.
16. Martinelli E., Paoli F., Gallot B., Galli G. Mesophase structure of low-wetting liquid crystalline polyacrylates with new perfluoroalkyl benzoate side groups, *J. Polym. Sci. Part A Polym. Chem.*, 48 (2010) 4128.
17. Abu-Sharkh B.F., Yahaya G.O., Ali S.A., Kazi I.W. Solution and interfacial behavior of hydrophobically modified water-soluble block copolymers of acrylamide and N-phenethylacrylamide, *J. Appl. Polym. Sci.*, 82 (2001) 467.
18. Hill J., Harris A. W., Manning M. et al. The effect of sodium chloride on the dissolution of calcium silicate hydrate gels, *Waste Manag.*, 26 (2006) 758.
19. Čapek L., Dědeček J., Wichterlová B. et al. Cu-ZSM-5 zeolite highly active in reduction of NO with decane, *Appl. Catal. B Environ.*, 60 (2005) 147.
20. Rahimi-Nasrabadi M., Maddah B., Shamsipur M., Moghimi A. NMR study of the stoichiometry and stability of 30-crown-10 complexes with Ca^{2+} , Sr^{2+} , Ba^{2+} and Pb^{2+} cations in acetonitrile-dimethylformamide binary mixtures, *J. Solution Chem.*, 43 (2014) 623.
21. Martins J.G., Pinto R.M., Gameiro P. et al. Aqueous equilibrium and solution structural studies of the interaction of N,N'-bis(4-imidazolymethyl)ethylenediamine with Ca(II), Cd(II), Co(II), Mg(II), Mn(II), Ni(II), Pb(II) and Zn(II) metal ions, *J. Solution Chem.*, 39 (2010) 1153.
22. Barros C.N., Arêas E.P.G., Figueiredo E.N., Arêas J.A.G. Low-resolution ^1H spin-spin relaxation of *n*-decane/water emulsions stabilized by beta-casein, *Colloids Surf. B. Biointerfaces*, 48 (2006) 119.
23. Rotureau E., Leonard M., Dellacherie E., Durand A. Amphiphilic derivatives of dextran: adsorption at air/water and oil/water interfaces, *J. Colloid Interface Sci.*, 279 (2004) 68.
24. Moradi M., Topchiy E., Lehmann T.E., Alvarado V. Impact of ionic strength on partitioning of naphthenic acids in water-crude oil systems – Determination through high-field NMR spectroscopy, *Fuel*, 112 (2013) 236.
25. Costa-Riu N., Maier E., Burkovski A. et al. Identification of an anion-specific channel in the cell wall of the Gram-positive bacterium *Corynebacterium glutamicum*, *Mol. Microbiol.*, 50 (2003) 1295.
26. Jung G., Redemann T., Kroll K. et al. Template-free self-assembling fullerene and lipopeptide conjugates of alamethicin form voltage-dependent ion channels of remarkable stability and activity, *J. Pept. Sci.*, 9 (2003) 784.
27. Lin J.C., Chuang W.H. Synthesis, surface characterization, and platelet reactivity evaluation for the self-assembled monolayer of alkanethiol with sulfonic acid functionality, *J. Biomed. Mater. Res.*, 51 (2000) 413.
28. Frasch H.F., Barbero A.M., Dotson G.S., Bunge A.L. Dermal permeation of 2-hydroxypropyl acrylate, a model water-miscible compound: effects of concentration, thermodynamic activity and skin hydration, *Int. J. Pharm.*, 460 (2014) 240.
29. Gun'ko V.M., Turov V.V., Krupska T.V. et al. Interfacial behavior of silicone oils interacting with nanosilica and silica gels, *J. Colloid Interface Sci.*, 394 (2013) 467.
30. Turov V.V., Gun'ko V.M., Zarko V.I. et al. Interfacial behavior of *n*-decane bound to weakly hydrated silica gel and nanosilica over a broad temperature range, *Langmuir*, 29 (2013) 4303.
31. Mitchell J., Webber J.B.W., Strange J.H. Nuclear magnetic resonance cryoporometry, *Phys. Rep.*, 461 (2008) 1.
32. Petrov O.V., Furó I. NMR cryoporometry: Principles, application and potential, *Progr. NMR Spectroscopy*, 54 (2009) 97.
33. Aksnes D.W., Forl K., Kimtys L. Pore size distribution in mesoporous materials as studied by ^1H NMR, *Phys. Chem. Chem. Phys.*, 3 (2001) 3203.
34. Gun'ko V.M., Turov V.V. Nuclear Magnetic Resonance Studies of Interfacial Phenomena, CRC Press, Boca Raton, 2013, 1006 p.
35. Gun'ko V.M., Skubiszewska-Zięba J., Leboda R. et al. Influence of morphology and composition of fumed oxides on changes in their structural and adsorptive characteristics

- on hydrothermal treatment at different temperatures, *J. Colloid Interface Sci.*, 269 (2004) 403.
36. *Gun'ko V.M., Leboda R., Skubiszewska-Zięba J. et al.* Structure of silica gel Si-60 and pyrocarbon/silica gel adsorbents thermally and hydrothermally treated, *Langmuir*, 17 (2001) 3148.
37. *Mironyuk I. F., Gun'ko V.M., Turov V. V. et al.* Characterization of fumed silicas and their interaction with water and dissolved proteins, *Colloids Surf. A: Physicochem. Eng. Aspects*, 180 (2001) 87.
38. *Gun'ko V.M., Turov V.V., Zarko V.I. et al.* Comparative characterization of polymethylsiloxane hydrogel and silylated fumed silica and silica gel, *J. Colloid Interface Sci.*, 308 (2007) 142.
39. *Frisch M. J., Trucks G. W., Schlegel H. B. et al.* Gaussian 09, Revision D.01, Gaussian, Inc., Wallingford CT, 2013.
40. *Stewart J.J.P.* MOPAC 2012, Colorado Springs, CO, Stewart Computational Chemistry, USA, <http://openmopac.net/>, 2014.
41. *Maia J.D.C., Carvalho G.A.U., Manguiera C.P. Jr. et al.* GPU linear algebra libraries and GPGPU programming for accelerating MOPAC semiempirical quantum chemistry calculations, *J. Chem. Theory Comput.*, 8 (2012) 3072.
42. *Marenich A.V., Cramer C.J., Truhlar D.G.* Universal solvation model based on solute electron density and on a continuum model of the solvent defined by the bulk dielectric constant and atomic surface tensions, *J. Phys. Chem. B*, 113 (2009) 6378.
43. *Schmidt M.W., Baldridge K.K., Boatz J.A. et al.* General atomic and molecular electronic structure system, *J. Comput. Chem.*, 14 (1993) 1347.
44. *Turov V.V., Gun'ko V.M., Turova A.A. et al.* Interfacial behavior of concentrated HCl solution and water clustered at a surface of nanosilica in weakly polar solvents media, *Colloids Surf. A: Physicochem. Eng. Aspects*, 390 (2011) 48.
45. *Gun'ko V.M., Morozova L.P., Turova A.A. et al.* Hydrated phosphorus oxyacids alone and adsorbed on nanosilica, *J. Colloid Interface Sci.*, 368 (2012) 263.

Received 31.07.2014, accepted 23.04.2015